



# Breathing responses produced by optogenetic stimulation of adrenergic C1 neurons are dependent on the connection with preBötzing complex in rats

Milene R. Malheiros-Lima<sup>1</sup> · Leonardo T. Totola<sup>1</sup> · Marlous V. G. Lana<sup>2</sup> · Bryan E. Strauss<sup>2</sup> · Ana C. Takakura<sup>3</sup> · Thiago S. Moreira<sup>1</sup>

Received: 26 February 2018 / Revised: 11 July 2018 / Accepted: 20 July 2018 / Published online: 27 July 2018  
© Springer-Verlag GmbH Germany, part of Springer Nature 2018

## Abstract

Optogenetic stimulation of the adrenergic C1 neurons produces cardiorespiratory activation, and selective depletion of these cells attenuates breathing responses induced by hypoxia. The preBötzing complex (preBötC) is a group of neurons located in the intermediate aspect of the ventrolateral medulla, critical for respiratory rhythmogenesis, and is modulated by glutamate and catecholamines. Our hypothesis is that selective activation of C1 neurons leads to breathing responses by excitatory connections with the preBötC neurons. Anatomical connection between C1 cells and preBötC was evaluated using retrograde (Cholera Toxin b; preBötC) and anterograde (LVV-PRsX8-ChR2-eYFP; C1 region) tracers. LVV-PRsX8-ChR2-eYFP (viral vector that expresses channelrhodopsin-2 (ChR2) under the control of the catecholaminergic neuron-preferring promoter (PRsX8) was also injected into the C1 region of male Wistar rats for the functional experiments. Anatomical results demonstrated that preBötC neurons receive projections from C1 cells, and these projections express tyrosine hydroxylase and vesicular glutamate transporter 2. Functional connection between C1 cells and preBötC was evaluated by photostimulation of ChR2-transduced C1 neurons before and after unilateral injection of the ionotropic glutamate antagonist, kynurenic acid (kyn), or cocktail of adrenergic antagonists in the preBötC. Kyn injection into preBötC blocked the increase in  $\text{Dia}_{\text{EMG}}$  frequency without changing the MAP increase elicited by photostimulation of C1 neurons, while the injection of adrenergic antagonists into the preBötC did not change  $\text{Dia}_{\text{EMG}}$  frequency and MAP increase induced by photostimulation of C1 cells. Our results suggest that the increase in breathing produced by photostimulation of C1 neurons can be caused by a direct glutamatergic activation of preBötC neurons.

**Keywords** Catecholamines · Glutamate · Hypoxia · Optogenetics · Rostrovventrolateral medulla · Ventilation

## Introduction

Adrenergic C1 cells, located in the rostral aspect ventrolateral medulla (RVLM), are classically known for their contribution

to cardiovascular control [22]. They use glutamate as a predominant transmitter, although they also synthesize catecholamines (i.e., dopamine, noradrenaline, and adrenaline) and express many neuropeptides [22, 51, 53]. C1 cells are activated by a variety of stimuli like hypoglycemia, infection or inflammation, hypotension, and hypoxia, being recently implicated in the control of these physiological processes [6, 22, 36, 47]. Optogenetics has been used as selective approach to study neuronal activation, including the C1 neurons. As these cells synthesize the transcription factor Phox2b, a viral vector that expresses the transgene under the control of the Phox2-responsive artificial promoter PRsX8 induces the expression of the light-gated cationic channel channelrhodopsin-2 (ChR2) in the C1 cells, making possible the manipulation of these cells by photostimulation [2, 30, 36, 60]. The selective stimulation of C1 cells causes a rise in blood pressure and

✉ Thiago S. Moreira  
tmoreira@icb.usp.br

<sup>1</sup> Department of Physiology and Biophysics, Institute of Biomedical Science, University of São Paulo, Av. Prof. Lineu Prestes, 1524, São Paulo, SP 05508-000, Brazil

<sup>2</sup> Center for Translational Investigation in Oncology/LIM24, Cancer Institute of São Paulo, University of São Paulo School of Medicine, São Paulo, SP 01246-000, Brazil

<sup>3</sup> Department of Pharmacology, Institute of Biomedical Science, University of São Paulo, São Paulo, SP 05508-000, Brazil

tachypnea, a smaller effect in tidal volume, and arousal from nonREM sleep and sighing, in both anesthetized and unanesthetized rodents [1, 4, 9, 30]. These effects caused by C1 stimulation mimic cardiorespiratory hypoxic responses [9].

Adrenergic C1 cells are highly collateralized and could contribute to hypoxic responses via connections with pontomedullary structures and sympathetic preganglionic neurons located in the intermediolateral column [10, 15, 22, 31, 32, 42, 55]. In the lower brainstem, C1 cells project to several noradrenergic neurons (e.g., A1, A2, A5, A6, and A7), to serotonergic neurons in the raphe, and to the dorsal motor nucleus of vagus [22]. In addition, there is evidence that RVLM catecholaminergic neurons could overlap with respiratory neurons [4, 9, 10, 31, 55], but confirmation of this connection is still pending. Thus, one of our hypotheses is that the axonal collateralization of C1 cells could overlap segments from the ventral respiratory column, contributing to the increase in breathing activity.

The preBötzing complex (preBötC), which is a component of the ventral respiratory column, is located in the intermediate portion of ventrolateral medulla (IVLM) [19, 22, 48, 49]. PreBötC is well known for its critical role in rhythmogenesis and in the control of inspiratory rhythm [16, 44, 48]. PreBötC neurons express neurokinin 1 receptors (NK1R) and somatostatin (STT), both used as a marker to identify the region [18–20, 46]. Several evidences indicate that preBötC modulates tachypnea and sighs, both affected by photostimulation or depletion of C1 cells [9, 35]. In addition, it is well known that preBötC neurons' activity is modulated by catecholamines and glutamate, both transmitters probably released by C1 cells [13, 43, 57, 58]. Therefore, our hypothesis is that preBötC receives catecholaminergic/glutamatergic inputs from C1 neurons, in order to contribute to the increase in breathing. Thus, the aims of our study were to evaluate if C1 cells project to preBötC neurons and if the breathing increase induced by optogenetic activation of C1 cells depends on glutamatergic and/or catecholaminergic receptors located in the preBötC region.

## Material and methods

### Animals

Experiments were performed in 20 adult male Wistar rats weighing 250–280 g, at the moment of the first surgery. The animals were housed individually in cages in a room with controlled temperature ( $24 \pm 2$  °C) and humidity ( $55 \pm 10\%$ ). Lights were on from 7:00 am to 7:00 pm. Standard Bio Base rat chow (Águas Frias, SC, Brazil) and tap water were available ad libitum. Animals were used in accordance with the guidelines approved by the Animal Experimentation Ethics Committee of the Institute of Biomedical Science at the University of São Paulo (protocol number 07/2014).

### Plasmid and virus preparation

The lentiviral vector was prepared using a previously described construct (pLenti-PRsX8-hChR2(H134R)-eYFP-WPRE; abbreviated PRsX8-ChR2-eYFP; all plasmids provided by Dr. R. Stornetta from University of Virginia) which features an enhanced version of the photoactivatable cationic channel ChR2 (H13R) fused to the fluorescent protein [1, 2, 30, 36]. Transgene expression was under the control of a synthetic phox2-selective promoter (PRsX8) [2–4, 8, 10, 30].

Briefly, pSPAX2 and VSV-g were used as the packaging plasmids and cotransfected with the PRsX8-ChR2-eYFP through the calcium phosphate precipitation method. Lentiviral supernatants were collected 24 and 48 h after transfection, followed by concentration by ultracentrifugation at 23,000 rpm during 90 min at 4 °C in a swinging bucket rotor (SW32Ti, Beckman Coulter, Brea, CA, USA). After centrifugation, medium was discarded, and pellet was resuspended in 25 µL of Hank's Balanced Salt Solution (Life Technologies, CA, USA), aliquoted, and stored in a  $-80$  °C freezer. We assessed virus titer by ELISA using the QuickTiter™Lentivirus Titer kit (Cell Biolabs, Inc., USA). The titer of the PRsX8-ChR2-eYFP lentivirus was  $6.75 \times 10^{11}$  (viral particles/ml).

### Injections of lentivirus into the rostral ventrolateral medulla

For the PRsX8-ChR2-eYFP virus injection, rats were anesthetized with a mixture of ketamine (100 mg/kg, ip.) and xylazine (7 mg/kg, ip.) and placed in a stereotaxic frame model 1760 (bite bar set at  $-3.5$  mm for flat skull; David Kopf Instruments Tujunga, CA, USA). The lentivirus was delivered by pressure through glass pipettes (20 µm) as previously described [2–4, 30]. For the anatomical experiments, the rats received only one unilateral injection of lentivirus within the left C1 region (100 nl over 5 min), while for the physiological experiments, the animals received two unilateral injections within the C1 region or in the RTN region (control experiment), (200 nl per site over 5 min). The injections were performed with 200 µm of distance between them. Stereotaxic coordinates to targeting C1 neurons were  $-2.8$  mm from lambda,  $\pm 1.8$  mm from midline, and  $-8.4$  mm from the skull surface. Stereotaxic coordinates to targeting RTN neurons were  $-2.6$  mm from lambda,  $\pm 1.8$  mm from midline, and  $-8.5$  mm from the skull surface. The coordinates and structures used to locate RVLM/C1 or RTN were based on the stereotaxic atlas for rats [40]. Animals used for optogenetic experiments were allowed to recover for 3 weeks before electrophysiological recordings, whereas animals used for neuronal tracing studies were killed 4 weeks after injection, to optimize the labeling of axonal projections. After surgery, the rats received a dose of antibiotic

ampicillin (benzylpenicillin, 160,000 U/kg), and analgesic (ketoprofen 0.6 mg/kg sc.).

### Injection of retrograde tracer into preBötzing complex

In three animals, preBötC injections of the retrograde tracer, Cholera Toxin b (CTb, 1% in deionized water; List Biological, Campbell, CA) were unilaterally performed. For preBötC injections, the dorsal surface of the brain was exposed via an occipital craniotomy. Stereotaxic coordinates to target the preBötC were  $-3.3$  mm from lambda,  $\pm 1.8$  mm from midline, and  $-8.0$  mm from the skull surface. The CTb (30 nl) was delivered by pressure through glass pipettes. Retrograde tracers were injected over 1 min, and the pipette remained in the tissue for at least 5 min to minimize movement of tracer up the injection tract. The pipette was then removed, and the incision site closed. The animals were allowed 7–10 days for surgical recovery and for transport of the retrograde tracer.

### Physiological preparation

The surgical procedures and experimental protocols were similar to those previously described (Wenker et al. 2013). Briefly, general anesthesia was induced with 5% halothane in 100% O<sub>2</sub>. A tracheostomy was made, and the halothane concentration was reduced to 1.4–1.5% until the end of surgery. The femoral artery was cannulated (polyethylene tubing, 0.6 mm o.d., 0.3 mm i.d., Scientific Commodities, Lake Havasu City, Arizona, USA) for measurement of arterial pressure (AP). The femoral vein was cannulated for administration of fluids and drugs. Photostimulation of C1 or RTN region and drugs injections into the preBötC were performed directly in the ventral medullary surface. For this, the rats were placed supine in the stereotaxic apparatus and all muscle and connective tissues covering the basilar surface of the occipital bone were removed. After this procedure, the anteroposterior extension from the vertebral arteries to the pontine nuclei was identified [37]. The diaphragm muscle was accessed by a ventral approach. To prevent any influence of artificial ventilation on diaphragm muscle activity (Dia<sub>EMG</sub>), the vagus nerve was bilaterally cut. Upon completion of the surgical procedures, halothane was replaced by urethane (1.2 g/kg, iv.) administered slowly. All rats were ventilated with 100% O<sub>2</sub> throughout the experiment. Rectal temperature was maintained at 37 °C. End-tidal CO<sub>2</sub> was monitored throughout each experiment with a capnometer (CWE, Inc., Ardmore, PA, USA) that was calibrated twice per experiment with a calibrated CO<sub>2</sub>/N<sub>2</sub> mix. This instrument provided a reading of  $<0.1\%$  CO<sub>2</sub> during inspiration in animals breathing 100% O<sub>2</sub> and provided an asymptotic, nearly horizontal reading during expiration. The adequacy of anesthesia was monitored during a 20-min stabilization period by testing for the absence of

withdrawal responses, pressor responses, and changes in diaphragm muscle activity (Dia<sub>EMG</sub>) to a firm toe pinch. Approximately hourly supplements of one third of the initial dose of urethane were needed to satisfy these criteria throughout the recording period.

### Photostimulation of the ventrolateral medulla

The light source was a diode pumped 473 nm blue laser (Crystal laser Model BC-473-060-M; Reno, NV, USA) controlled by a function generator Grass Technologies/Astro-Med Inc., Warwick, RI, USA) to generate 10 ms light pulses. Stimulation trials generally consisted of 10–30 s trains for 10 ms pulses delivered at 20 Hz. The actual power output measured at the end of fiber optic with a light meter (Thorlabs, Newton, NJ, USA) was close to 9 mW. The same fiber optic was used for all experiments [2, 30]. To verify the effect of co-transfection of RTN cells on the cardiorespiratory responses, the photostimulation of RTN region was performed in all rats subjected to lentivirus injection into C1 regions.

### Physiological variables

As previously described, mean arterial pressure (MAP), diaphragm muscle activity (Dia<sub>EMG</sub>), and end-expiratory CO<sub>2</sub> (etCO<sub>2</sub>) were digitized with a micro1401 (Cambridge Electronic Design), stored on a computer, and processed offline with version 6 of Spike 2 software (Cambridge Electronic Design, Cambridge, UK). Integrated diaphragm muscle activity ( $\int$ Dia<sub>EMG</sub>) was obtained after rectification and smoothing ( $\tau = 0.015$  s) of the original signal, which was acquired with a 30–300 Hz bandpass filter. Dia<sub>EMG</sub> amplitude, Dia<sub>EMG</sub> frequency, and MAP were evaluated before and after pharmacological administration and during photostimulation.

### Drugs

All drugs were purchased from Sigma Aldrich (Sigma Chemicals Co.) unless otherwise stated. Kynurenic acid, a non-selective ionotropic glutamatergic antagonist (100 mM–50 nl first dissolved in 1 N NaOH and then diluted in phosphate-buffered saline pH 7.4), prazosin hydrochloride ( $\alpha_1$ -AR antagonist, 6 pmol/30 nl in propylene glycol pH 7.4), yohimbine hydrochloride ( $\alpha_2$ -AR antagonist, 3 pmol/30 nl in propylene glycol pH 7.4), and propranolol hydrochloride ( $\beta$ -AR antagonist, 3 pmol/30 nl in sterile saline pH 7.4) were pressure injected (Picospritzer III, Parker Hannifin) (30 nl in 3 s) through single-barrel glass pipettes (20- $\mu$ m tip diameter) [39]. Injections of CTb into the preBötC were placed  $-3.3$  mm from lambda,  $\pm 1.8$  mm from midline, and  $-8.0$  mm from the skull surface. Pharmacological injections into the PreBötC were performed using the ventral approach to access the medulla surface. The pipettes were placed using the most rostral

root of the hypoglossal nerve (RRXII) as reference, being performed 750  $\mu\text{m}$  caudal from RRXII, 2 mm lateral to the midline, and 700  $\mu\text{m}$  dorsal to the ventral medullary surface [29].

All drugs contained a 5% dilution of fluorescent latex microbeads (Lumafluor, New City, NY, USA) for later histological identification of the injection sites. Complete recovery from the respiratory effects of the antagonists occurred within 45–60 min.

## Histology

At the end of the physiological or anatomical procedures, the rats were deeply anesthetized (5% halothane or pentobarbital; 60 mg/kg, ip., respectively). They were immediately perfused with a heparin solution (500 units, intracardially) followed by a phosphate-buffered saline (PB—pH 7.4) and 4% phosphate-buffered paraformaldehyde (0.1 M, pH 7.4). After 4 h of postfixation, the brains were cryoprotected by overnight immersion in a 20% sucrose solution (20% glycerol plus 30% ethylene glycol in 50 mM phosphate buffer, pH 7.4) and 40- $\mu\text{m}$ -thick sections were cut using a sliding microtome.

All histochemical procedures were done using free-floating sections according to previously described protocols [35]. Briefly, the primary antibodies were diluted in PB containing 1% normal donkey serum (017-000-121, Jackson Immuno Research Laboratories) and 0.3% Triton X-100 and incubated for 24 h. Tyrosine hydroxylase (TH) immunoreactivity was detected using mouse anti-TH (1:1000; Chemicon, Temecula, CA, USA), followed by goat anti-mouse Cy3 or Alexa488 IgG (1:200; Jackson Laboratories; West Grove, PA, USA). ChR2-eYFP was detected by enhanced green fluorescent protein (eGFP) immunoreactivity, using chicken anti-GFP antibody (1:2000; Sigma, St. Louis, MO, USA), followed by donkey anti-chicken Cy3 IgG (1:200; Jackson Laboratories, West Grove, PA, USA). Cholera Toxin b (CTb) immunoreactivity was detected using goat anti-CTb (1:1000; Chemicon, Temecula, CA, USA), followed by goat anti-mouse Cy3 IgG (1:200; Jackson Laboratories, West Grove, PA, USA). Vesicular glutamate transporter 2 (VGlu2, Slc17a6) pig anti-VGlu2 antibody (AB 5907; 1:2000 dilution; Chemicon International, Temecula, CA, USA), followed by donkey anti-guinea pig Cy3 IgG (1:200; Jackson Laboratories, West Grove, PA, USA). The sections were mounted on gelatin-coated slides, coverslipped with DPX (Aldrich, Milwaukee, WI, USA).

## Cell counting, imaging and data analysis

A multifunction microscope, Zeiss Axioimager A1 microscope (Zeiss, Muenchen, Germany), was used to image sections and perform subsequent analyses. Immunofluorescence was examined under epifluorescence illumination.

The locations of TH, eYFP, and CTb into the ventrolateral medulla [C1 region (6 sections/animal: between –11.60 and

12.80 mm from bregma), RTN region (7 sections/animal: between –10.16 and –11.60 mm from bregma), and PreBötC (2 sections/animal: between –12.80 and 13.04 mm from bregma)] and dorsal medulla [nucleus of the solitary tract—NTS (5 sections/animal: between –13.52 and 14.48 mm from bregma)] were plotted 1:6 sections [40]. The profile counts of animals that receive PRSx8-ChR2-eYFP or CTb injections reflected only one side of the medulla and were compared with the control rats.

Digital color photomicrographs were acquired using a Zeiss Axioacam HRc camera. Images of double immunofluorescence stained sections were acquired and analyzed with the Axiovision software (Zeiss), which permits the acquisition of images from several separate fluorescence channels. Image J (version 1.41; National Institutes of Health, Bethesda, MD) was used for cell counting and Canvas software (ACD Systems, Victoria, Canada, v. 9.0) was used for line drawings. The neuroanatomical nomenclature employed during experimentation was described relative to the caudal pole of the facial motor nucleus (bregma = –11.6 mm) and was also confirmed by Paxinos and Watson [40]. Confocal images (Carl Zeiss, Jena, Germany) were used to evaluate the colocalization between axonal varicosities of eYFP and VGlu2 or TH in the preBötC region. Terminal fields were mapped using a  $\times 63$  oil-immersion objective by taking 0.3  $\mu\text{m}$  z-stack images of both red and green fluorescence through the tissue where discernible eYFP-labeled fibers were sharply in focus. These stacks were usually between 5 and 10  $\mu\text{m}$  in depth. Terminals were marked as positive only where both eYFP and VGlu2 or TH immunofluorescent profiles were in focus in at least 2 consecutive z sections.

## Statistics

Data normality was assessed using the Shapiro-Wilk test, and the normally distributed data were expressed as means  $\pm$  SEM. The data regarding number of neurons were compared between groups and across bregma levels points using two-way ANOVA, with repeated measures. When applicable, the Student Newman Keuls post hoc test was used. Inter-group differences before and after drugs administration were evaluated with one-way ANOVA with repeated measures. Significance level was  $p < 0.05$ .

## Results

### PreBötzing projecting catecholaminergic neurons in the C1 region

Three cases with CTb injections within the preBötC were analyzed to visualize retrograde labeling in the C1 region (Figs. 1a, c and 2a). The distribution of representative CTb

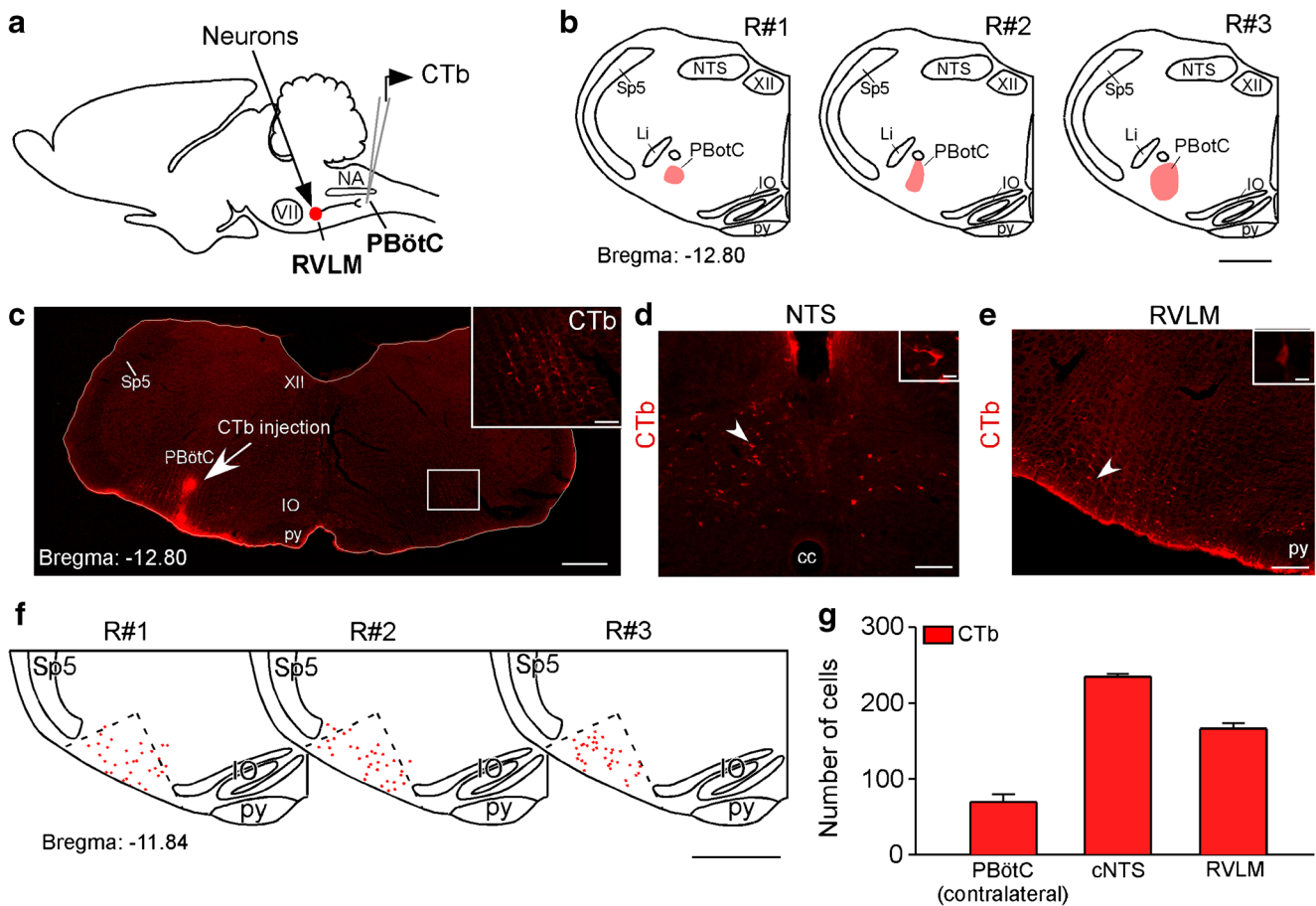


**Fig. 1** Projections from C1 region to preBotC revealed by retrograde tracer cholera toxin b (CTb). **a** Experimental design. **b** Schematic drawing of coronal sections showing the three injections of CTb confined to the preBotC region (12.80 mm caudal to bregma level; according to [40]). **c** Photomicrograph showing the typical injection site of the retrograde tracer CTb in the preBotC region. The inset shows CTb-labeled neurons in contralateral side of preBotC region. **d** CTb-labeled neurons in commissural nucleus of solitary tract (cNTS). **e** CTb-labeled neurons in C1 region. **f** Schematic drawing of a coronal section showing the distribution of CTb neurons in C1 region (11.84 mm caudal to bregma

level; according to Paxinos and Watson atlas, 2007). **g** Total number of CTb-labeled cells in the preBotC, cNTS, and C1 regions (mean ± SEM of three rats). The neurons were counted per section in a one-in-six series of 40  $\mu$ m in coronal sections of three rats. Scale bar in **b**, **c**, and **f** = 1 mm; **d** = 0.5 mm/10  $\mu$ m; **e** = 0.5 mm/10  $\mu$ m. NA, nucleus ambiguus; IO, inferior olive; Li, nucleus linearis; NTS, nucleus of the solitary tract; cNTS, commissural nucleus of the solitary tract; preBotC, preBötzinger Complex; py, pyramid; RVLM, rostral ventrolateral medulla; Sp5, spinal trigeminal tract; VII, facial motor nucleus

injections centered on the preBotC of three rats is shown in Fig. 1b, c. C1 neurons with projections to preBotC were labeled with CTb 7 to 10 days before the rats were sacrificed. TH immunoreactivity was used to identify C1 neurons (Fig. 2). To characterize the C1 neurons that project to preBotC, a series of 40- $\mu$ m-thick coronal were analyzed and cells were counted in only six levels of the C1 region: -11.6 to -12.80 mm relative to bregma, in order to include the lowest possible amount of catecholaminergic neurons in the A1 neurons. A considerably high number of retrograde labeled neurons (CTb<sup>+</sup>) were found in the C1 region (Figs. 1e–g and 2b), particularly in more rostral regions of the C1 region. For example, we found from a total of  $104 \pm 14$  TH-ir cells in the C1 region,  $29 \pm 4$  neurons project to preBotC, representing 28% of TH cells in the C1 region (Figs. 1d, g and 2b–e). As expected, CTb expression was also observed in

cell bodies located in the contralateral preBotC site (Fig. 1c). CTb-labeled neurons were less numerous in the preBotC and C1 region than in dorsal region of the brainstem such as the nucleus of the solitary tract (NTS) (Fig. 1d, g).

### PreBötzinger targeted by Chr2-expressing catecholaminergic C1 neurons

The second series of experiment was designed to identify the presence of axonal varicosities in the preBotC, a region that harbors the vast majority of inspiratory rhythm generator neurons [48]. Injections of the lentivirus PRSx8-ChR2-eYFP into the left C1 region produced intense fluorescence protein expression only in neurons (Fig. 3a–f). These neurons (TH<sup>+</sup>/eYFP<sup>+</sup>) were always located in close proximity to the original injection site and were concentrated in the region of the

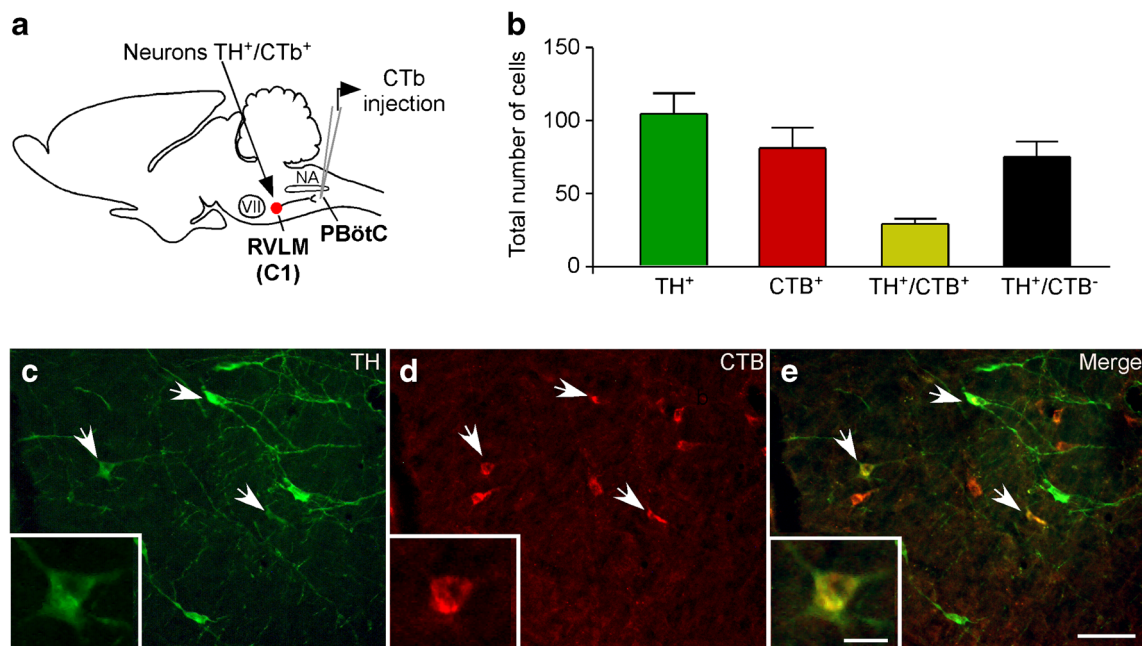


**Fig. 2** Projections from adrenergic C1 neurons to preBotC revealed by retrograde tracer cholera toxin b (CTb) and tyrosine hydroxylase (TH). **a** Experimental design. **b** Total number of CTb and/or TH-labeled cells in the C1 region (mean  $\pm$  SEM of three rats). The neurons were counted per section in a one-in-six series of 40  $\mu$ m in coronal sections of three rats (6 sections for C1 region). **c–e** Representative photomicrography of one rat

with CTb injection into the C1 region. **c** Catecholaminergic neurons (TH). **d** CTb-labeled cells. **e** Merged photomicrography of CTb and TH shows that most of the labeled cells are catecholaminergic (arrows). Scale bar in **e** = 0.5 mm/10  $\mu$ m. NA, nucleus ambiguus; IO, inferior olive; preBötC, preBötzinger Complex; VII, facial motor nucleus

ventrolateral reticular formation that lies below the caudal end of the facial motor nucleus and extends up to 500  $\mu$ m posterior to this level (–11.6 to –12.8 mm caudal to Bregma; Fig. 3b, c). This region contains the bulk of the C1 and other blood pressure-regulating presympathetic neurons [45, 60]. Smaller injections were performed to avoid the transduction of the retrotrapezoid nucleus (RTN) and A1 region (Fig. 3g–i). Figure 3b, c shows the average rostro-caudal distribution of TH-positive and TH-negative neurons expressing eYFP for 3 rats used in the anatomical experiments (Fig. 1b) and 14 rats used in the physiological experiments (Fig. 1c). On average,  $52 \pm 4\%$  of the eYFP-positive neurons were immunoreactive (ir) for TH in anatomical experiments, while  $77 \pm 3\%$  of the eYFP-positive neurons were immunoreactive (ir) for TH in physiological experiments.

Transduced catecholaminergic neurons had putative catecholaminergic and glutamatergic varicosities within the preBötC (Fig. 4a–i). We also noticed that every pontomedullary region that harbors noradrenergic neurons including the locus coeruleus, A1, A2, and A5 region also have eYFP-labeled fibers (data not shown; [4]). We observed light projections within the medullary raphe, a region also noted for its role in respiratory control [11, 24], moderately dense projections to the nucleus of the solitary tract which receives input from the carotid bodies and other cardiopulmonary afferents [34], and extremely dense projections to the dorsal motor nucleus of the vagus [12]. All projections had a strong ipsilateral predominance.

### Inhibition of ionotropic glutamatergic receptors into preBötzinger reduces the breathing increase induced by optogenetic activation of C1 cells

Photostimulation of the RVLM (30 s; 20 Hz, 10 ms pulses, 7–10 mW,  $N = 7$ ; Fig. 5a, b), containing Chr2-expressing neurons, raised MAP ( $133 \pm 7$ , vs. baseline  $118 \pm 6$  mmHg,  $p < 0.01$ ) and the  $\text{Dia}_{\text{EMG}}$  frequency ( $49 \pm 1$ , vs. baseline  $42 \pm 1$  breaths/min,  $p < 0.05$ ), without changing  $\text{Dia}_{\text{EMG}}$  amplitude (Fig. 6a–c). Typically, MAP increased steadily over time and reached a maximum towards the end of the stimulus. The  $\text{Dia}_{\text{EMG}}$  frequency response consisted of an initial burst at the onset of the stimulus period that was followed by a steady-state discharge greater than the resting level. At the end of the stimulus,  $\text{Dia}_{\text{EMG}}$  frequency decreased abruptly then recovered gradually as MAP returned to the prestimulus level (Fig. 6a). This undershoot in MAP is presumably due to baroreceptor feedback [2].

Figure 6a, c shows a representative tracer of the photostimulation of RTN region of one rat subjected to PRSx8-ChR2-eYFP injection into C1 neurons, demonstrating that a small transfection of RTN region was not able to elicit an increase in breathing ( $42 \pm 1$ , vs. baseline  $41 \pm 1$  bpm,  $p = 0.698$ ) or blood pressure ( $117 \pm 6$ , vs. baseline  $115 \pm 5$  mmHg,  $p = 0.724$ ). The effect is completely different when the stimulation is on the C1 region (Fig. 6a–c). In addition, as expected, when the transfection target the RTN region, we noticed that

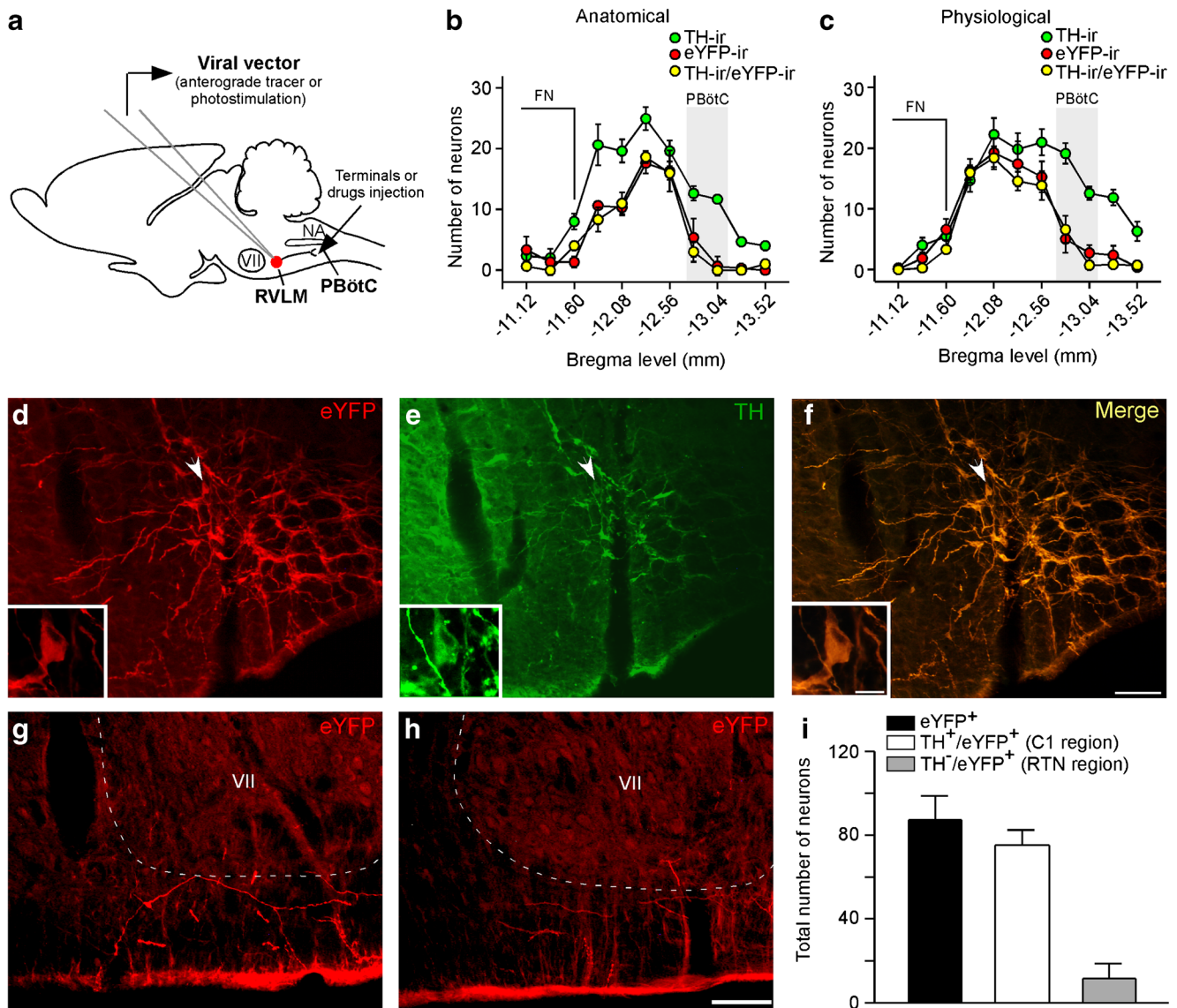


**Fig. 3** Catecholaminergic C1 neurons project to preBötC. **a** Experimental design. **b, c** Rostral caudal distribution of Chr2-eYFP-transduced neurons used in anatomical ( $N=3$ ) and physiological experiments ( $N=14$ ), respectively. The number of transduced catecholaminergic neurons (TH<sup>+</sup>/eYFP<sup>+</sup>) and transduced neurons without tyrosine hydroxylase or eYFP was counted per section in a one-in-six series of 40  $\mu$ m in coronal sections. FN shows the location of the facial motor nucleus. **d–f** Representative photomicrography of one rat transduced by PRSx8-

Chr2-eYFP in C1 region. **d** Transduced (eYFP), **e** catecholaminergic neurons (TH) and **f** merged photomicrography of eYFP and TH shows that transduced cells are catecholaminergic. Note the overlap of eYFP and TH (arrows). **g, h** Representative photomicrographs showing the distribution of fibers and terminals that express eYFP derive from C1 in the RTN region. **i** Summary data showing the total number of eYFP and/or TH-labeled cells in the ventrolateral medulla. Scale bar in **f** = 0.5 mm/10  $\mu$ m; scale bar in **f** and **h** = 100  $\mu$ m. VII, facial motor nucleus

laser stimulation produced a massive increase in breathing frequency by up to  $52 \pm 13\%$  ( $p=0.012$ ), and amplitude by  $76 \pm 16$  ( $p=0.0049$ ) without changing blood pressure ( $119 \pm 6$ , vs. baseline  $120 \pm 3$  mmHg,  $p=0.914$ ) (data not shown) [1].

Considering that we have a significant input from C1 to the preBötC (Figs. 2 and 4), our next set of experiments was to determine if the increase in breathing elicited by photostimulation is dependent on glutamatergic input into the preBötC (Fig. 5a, b). The injection sites of saline or the broad spectrum ionotropic glutamatergic antagonist kynurenic acid (100 mM–50 nl) into the preBötC were thoroughly

evaluated (Fig. 5c, d). The brainstem location of photostimulation and preBötC injections are demonstrated in Fig. 5a, and the experimental protocol in Fig. 5b. As showed by Fig. 5a, b, all rats were subjected to two consecutive stimulations of C1 region, with 15 min of interval between them, before and after the saline or kyn injection into preBötC (Fig. 5b–d). As expected, photostimulation of C1 cells increased MAP and Dia<sub>EMG</sub> frequency, and the saline injection into preBötC did not change these responses (Fig. 6a, b). In contrast, 10 min after Kyn injection into preBötC, the Dia<sub>EMG</sub> amplitude was reduced and the Dia<sub>EMG</sub> frequency was

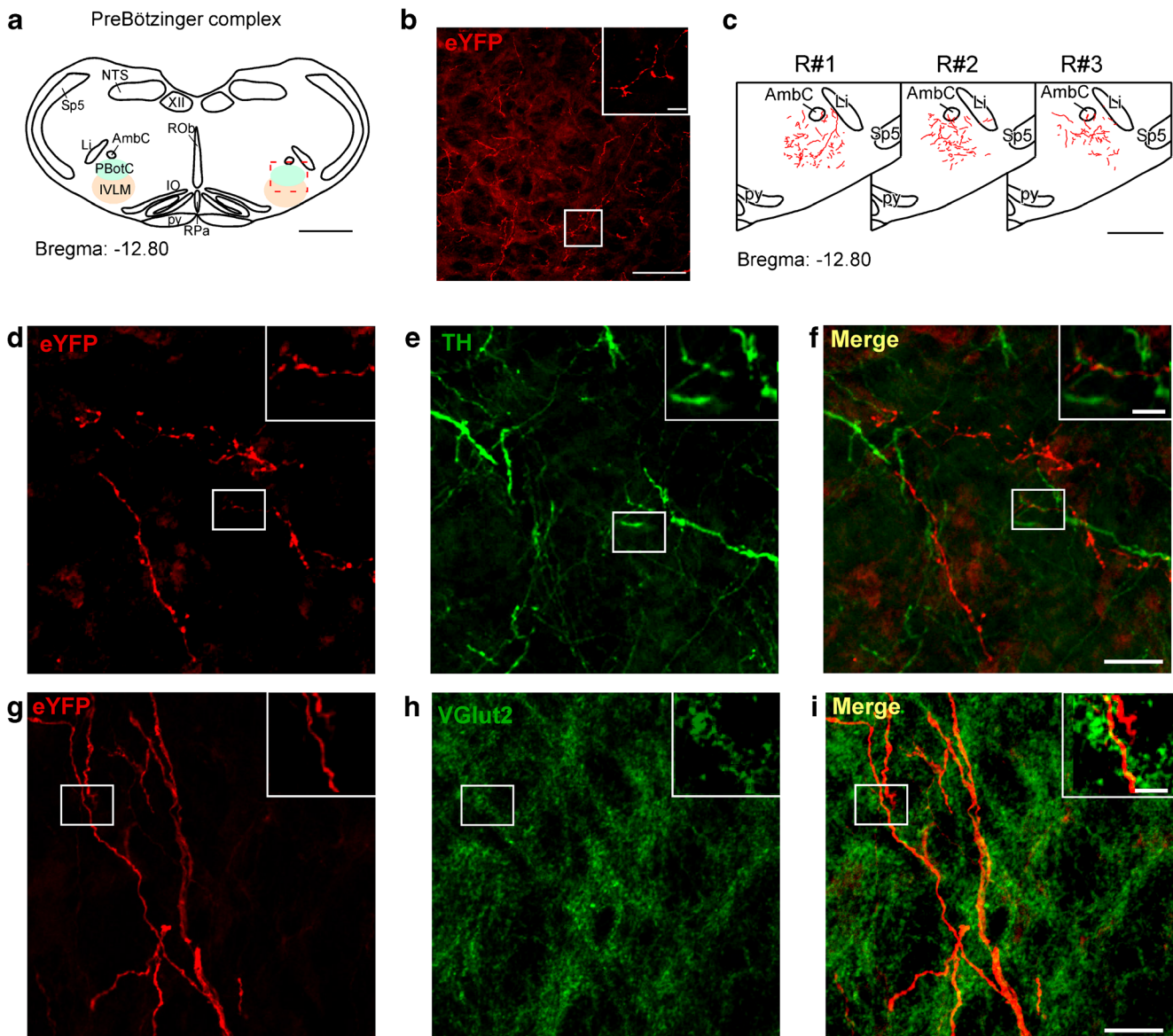


**Fig. 4** PreBötC varicosities from C1 neurons are glutamatergic and catecholaminergic. **a** Location of preBötC (12.80 mm caudal to bregma level). **b** Representative photomicrograph showing the distribution of fibers and terminals that express eYFP derived from C1 in the preBötC region. **c** Schematic drawing showing the distribution of fibers and terminals that express eYFP within the preBötC region in three rats. **d, g** Representative photomicrography showing the distribution of fibers and terminals that express eYFP derived from C1 cells in the preBötC region. **e, h** Catecholaminergic (TH) or glutamatergic (VGlut2) fibers

and/or terminals in preBötC region. **f, i** Merged photomicrography of eYFP and TH or eYFP and VGlut2 shows that transduced fibers and terminals in preBotC region are catecholaminergic and glutamatergic. Scale bar in **a** and **c** = 1 mm; **b** = 100/10  $\mu$ m; **f** and **i** = 10/0.5  $\mu$ m. AmbC, nucleus ambiguus; IO, inferior olive; Li, nucleus linearis; NTS, nucleus of the solitary tract; preBötC, preBötzing Complex; py, pyramidal; RPa, raphe pallidus; RVLM, rostral ventrolateral medulla; Sp5, spinal trigeminal tract; VII, facial motor nucleus

increased, without affecting MAP (Fig. 6a, e). Photostimulation of C1 cells after kyn injection into preBötC reduced the increase in  $\text{Dia}_{\text{EMG}}$  frequency ( $2 \pm 1$  vs. saline + laser  $25 \pm 5\%$ ,  $p = 0.002$ ), but did not affect the increase in MAP ( $p > 0.05$ ) (Fig. 6a–c). These results suggest that ionotropic glutamatergic receptors, located in the preBötC region, contribute to the breathing increase induced by optogenetic stimulation of C1 cells.

### Blockade of adrenergic receptors into preBötC did not affect the breathing response induced by optogenetic activation of C1 cells

It is well known that preBötC neurons' activity is modulated by catecholaminergic inputs [58–59]. Therefore, the next step was to further evaluate the potential involvement of  $\alpha 1$ -,  $\alpha 2$ , and  $\beta$ -ARs in the respiratory response produced by



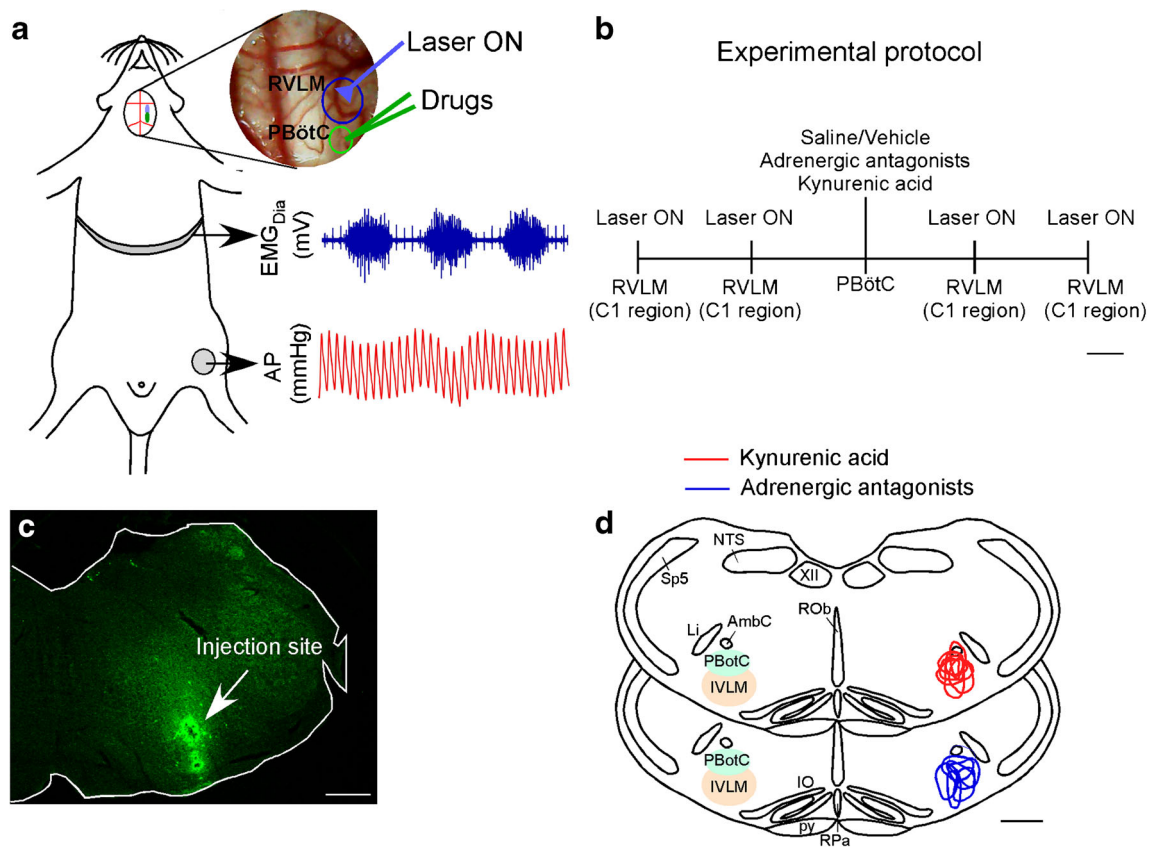


**Fig. 5** Injection site of PRSx8-ChR2-eYFP targeting C1 neurons and injection site targeting the preBötC in rats used to optogenetic experiments. **a, b** Experimental design. **c** Photomicrography showing the typical injection sites in the preBötC region. **d** Injection sites of kynurenic acid or adrenergic antagonists into preBötC (12.80 mm caudal to bregma

level). Scale bar in **c** and **d** = 1 mm. AmbC, nucleus ambiguus; IO, inferior olive; IVLM, intermediate ventrolateral medulla; Li, nucleus linearis; NTS, nucleus of the solitary tract; preBötC, preBötzinger Complex; py, pyramid; RVLM, rostral ventrolateral medulla; Sp5, spinal trigeminal tract

photostimulation of the C1 region (Fig. 5b–d). We found that preBötC injections of adrenergic antagonists cocktail with prazosin hydrochloride ( $\alpha_1$ -AR antagonist, 6 pmol/30 nl), yohimbine hydrochloride ( $\alpha_2$ -AR antagonist, 3 pmol/30 nl), and propranolol hydrochloride ( $\beta$ -AR antagonist, 3 pmol/30 nl) did not significantly affect photostimulation-mediated activation of respiratory frequency ( $53 \pm 2$  vs. saline + photostimulation  $50 \pm 2$  breaths/min,  $p = 0.217$ ) and the increase in MAP ( $129 \pm 7$  vs. saline + photostimulation  $131 \pm 4$  mmHg,  $p = 0.699$ ) (Fig. 6a–c).

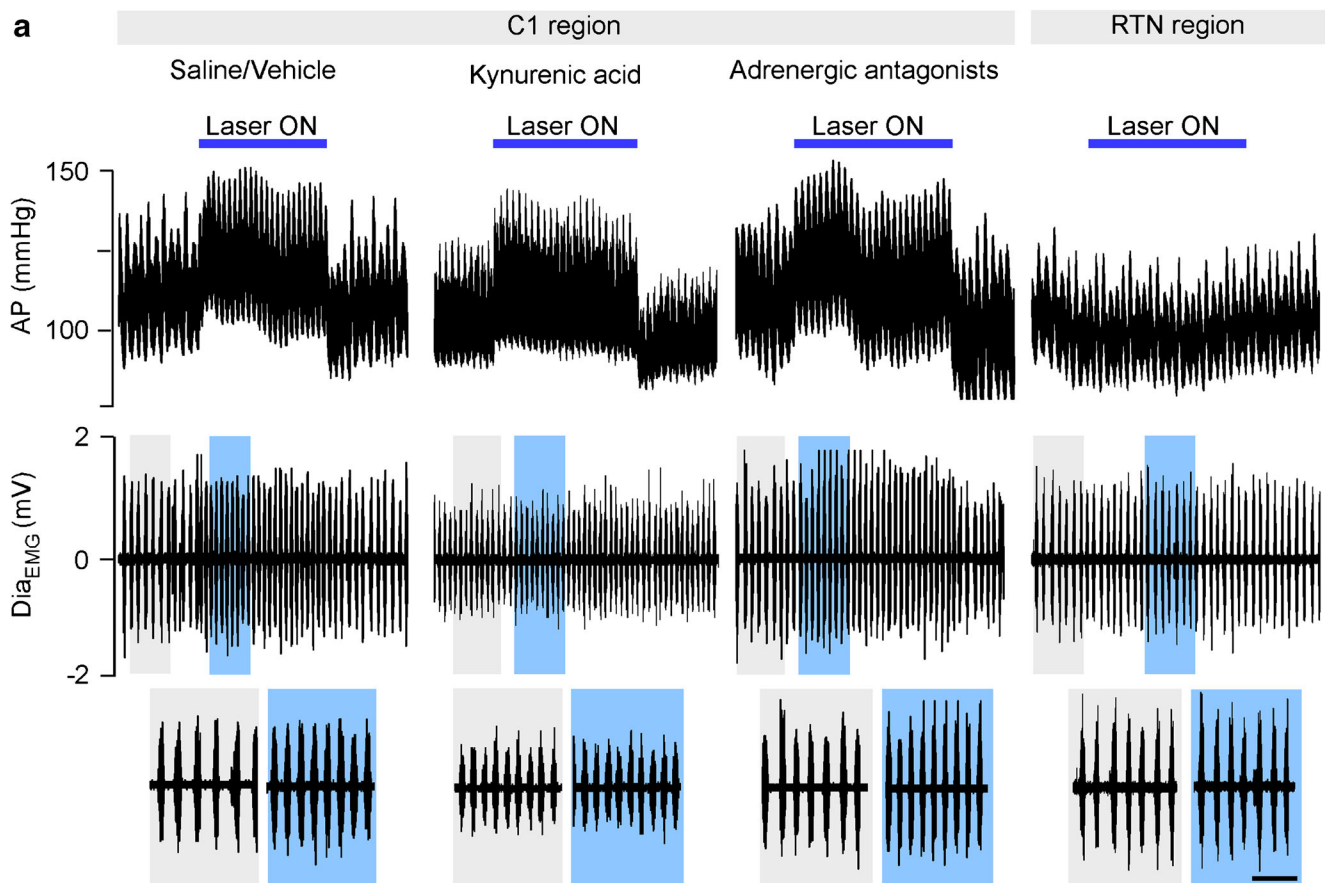
## Discussion

In the present study, we evaluated the structural and functional connections between catecholaminergic C1 cells and the preBötC. Our findings provide evidence to support a direct connection between both regions, suggesting a synergic activity between respiratory and cardiovascular system. The structural evaluations show fibers and terminals double-labeled with eYFP and either TH or VGlu2 in the preBötC region of rats subjected to injection of a selective anterograde tracer into

C1 region. These results allow us to suggest that there is a structural connection between C1 and preBötC. In addition, cell bodies ( $CTb^+/TH^+$ ) were found in C1 region, reinforcing our previous evidence of the connection between both regions. In the functional experiments, the photostimulation of C1 cells increased blood pressure and breathing frequency, confirming previous results from literature [9]. The blockade of ionotropic glutamatergic receptors, but not the  $\alpha$ - and  $\beta$ -adrenergic receptors, into preBötC ablated the increase in breathing frequency elicited by photostimulation of C1 cells, without affecting the pressor response. Thus, the anatomical and functional connections between C1 and preBötC could contribute for the breathing increase induced by selective stimulation of C1 cells, presumably using glutamate as a neurotransmitter.

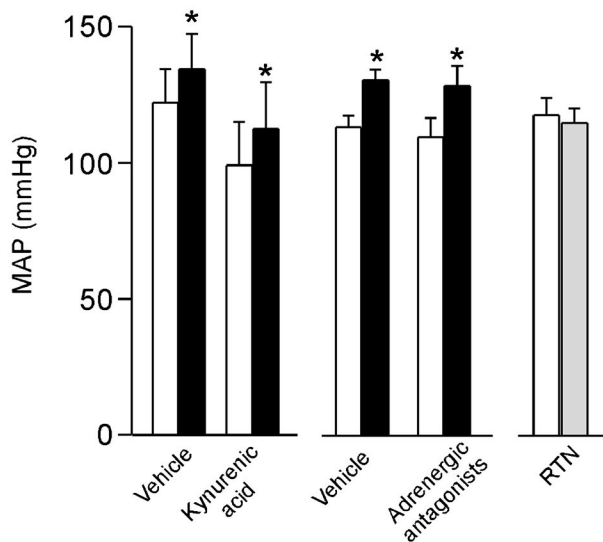
## Catecholaminergic C1 neurons project to preBötC

Several fibers and varicosities were observed in the preBötC region (Fig. 4). The extension of our transductions was restricted to C1 region, indicating that eYFP fibers and terminals located in the preBötC belong to C1 neurons residing in the RVLM. However, we cannot exclude the possibility that a

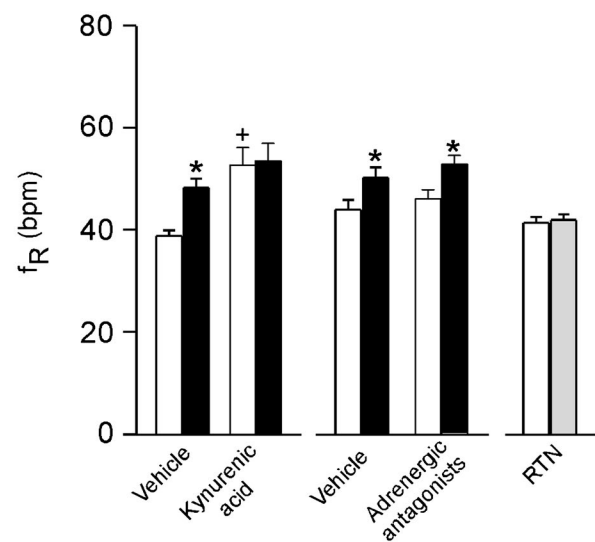


**b**

□ Basal  
 ■ Photostimulation: C1 region  
 ▨ Photostimulation: RTN region



**c**



small number of Phox2b neurons from retrotrapezoid nucleus (RTN) or noradrenergic A1 region may be contributing to these responses [27, 56, 62]. Catecholaminergic neurons from A2/C2, A5, and A6 project to C1 region and medullary respiratory network [14, 23, 58]. Therefore, the fibers and terminals

only labeled with TH in the preBötC observed in our study could derive from other catecholaminergic regions. The strongest evidence that C1 neurons in fact project to preBötC is the presence of eYFP and TH double-labeling in this region. TH and CTb double-labeling in the C1 region,

◀ **Fig. 6** Inhibition of ionotropic glutamatergic receptors into preBötC abolishes the increase of breathing elicited by selective stimulation of C1 cells. **a** Representative recordings from one rat showing that photostimulation of C1 region before and after unilateral injection of saline, kynurenic acid (kyn), or cocktail of adrenergic antagonists into preBötC. Representative recording showing photostimulation of RTN region in C1 transfected rats. Note that the kyn abolishes the increase of breathing elicited by photostimulation (Laser ON) but did not change the increase in mean arterial pressure (MAP). **b** Changes in mean arterial pressure (MAP, mmHg) elicited by optogenetic stimulation of C1 cells (laser ON 30 s; 20 Hz, 10 ms pulses, 7–10 mW) before and after the injection of saline/vehicle, kynurenic acid (100 mM–50 nl) or cocktail of adrenergic antagonists [prazosin hydrochloride ( $\alpha_1$ -AR antagonist, 6 pmol/30 nl) + propranolol hydrochloride ( $\beta$ -AR antagonist, 3 pmol/30 nl) + yohimbine hydrochloride ( $\alpha_2$ -AR antagonist, 3 pmol/30 nl)], and elicited by optogenetic stimulation of the RTN region **(c)** changes in diaphragm frequency ( $f_R$ , breaths per min - bpm) elicited by optogenetic stimulation of C1 cells before and after the injection of saline/vehicle, kynurenic acid or cocktail of adrenergic antagonists, and induced by photostimulation of the RTN region. \*different from baseline ( $p < 0.05$ ); +different from saline treatment ( $p < 0.05$ ).  $N = 7$ –14/group of rats

observed in rats that received retrograde tracer injection (CTb) into preBötC, reinforce our hypothesis. Our results agree with a recent study, which demonstrated that synaptic terminals expressing D $\beta$ H connect with neurons in the preBötC region [31]. Different from Kang and colleagues [31], we used a selective viral vector as an anterograde tracer, showing direct evidence that C1 projects to preBötC.

Previous studies demonstrated that C1 neurons express VGlut2, catecholamines, and several neuropeptides (neuropeptide Y, substance P, enkephalins, and thyrotropin-releasing hormone) [7, 22, 55]. In agreement with this information, we also confirmed that the eYFP-labeled fibers and terminals located in the preBötC express both TH and VGlut2. Therefore, our results show that C1 neurons project to preBötC and suggest that they could modulate the preBötC activity by releasing both glutamate and catecholamines.

### Glutamatergic, but not adrenergic, receptors in the preBötC modulate the breathing increase induced by optogenetic activation of C1 cells

The C1 neurons arborize within the ventral respiratory column region [10, 55]. Glutamate injections into preBötC increase breathing, and the activation of  $\beta$ -adrenergic receptors in this region generates sighs [50, 59]. Previous studies demonstrated that the selective activations of C1 cells mimic several effects elicited by hypoxia [2, 4, 9]. We and others have accumulated several evidences for a role of C1 neurons in breathing control [4, 5, 9, 30, 35, 36]. We showed that selective ablation of C1 neurons reduces the increase in breathing frequency elicited by hypoxia [35]. In the present study, we added one more piece to this puzzle demonstrating that breathing activation elicited by photostimulation of C1 cells is dependent on

glutamatergic synapses within the preBötC region, presumably via direct connections.

The preBötC is a bilateral cluster of functionally heterogeneous neurons, including glutamatergic neurons and high levels of NK1R and somatostatin expression located just ventral to the nucleus ambiguus in the intermediate aspect of the ventrolateral medulla [18, 21, 53]. Bilateral ablation of preBötC neurons leads to a progressive and irreversible disruption in breathing pattern [19, 20, 48]. Here, we performed unilateral pharmacological blockade of the preBötC in order to avoid disruption in the breathing pattern. In our study, we noticed a slight increase in breathing frequency after kynurenic acid injection into the preBötC, probably due to a compensation of the preBötC neurons from the contralateral site. This effect is consistent with a previous work from Dr. Feldman's laboratory suggesting that unilateral ablation of preBötC neurons leads to breathing impairment [17]. Although the inherent limitation of our experimental protocol, i.e., increase in breathing frequency triggered by unilateral injection of kynurenic acid into preBötC, we are demonstrating evidence that physiological responses caused by C1 activation are mediated by glutamate release. In agreement with our data, genetic deletion of VGlut2 from dopamine- $\beta$ -hydroxylase-expressing neurons of the rostral ventrolateral medulla of mice was able to blockade the increase of breathing frequency produced by photostimulation of C1 neurons [5]. In addition, there is evidence that the physiological responses elicited by C1 cells activation are dependent on glutamate release [5, 12, 26]. In anesthetized rats, the photostimulation of C1 cells induces only a moderate increase in breathing frequency. Thus, we cannot exclude the possibility that the photostimulation of C1 cells is not enough to increase breathing when the baseline breathing frequency is high in anesthetized rats.

We did not observe any changes in resting MAP after kynurenic acid injection into preBötC. In addition, inhibition of ionotropic glutamatergic receptors in this region did not change the MAP increase induced by photostimulation of C1 cells. It is important to highlight that the inhibition of glutamatergic inputs to CVLM should increase the blood pressure, while in IVLM or RVLM, any changes in blood pressure are expected [33, 38].

Our work, taken together with previous work from others, indicates that catecholaminergic neurons in the C1 region use glutamate primarily, if not exclusively, as a transmitter to influence downstream autonomic and/or respiratory neurons [5, 36].

### Selectivity of the lentiviral vector and limitations of the optogenetic methodology

The PRSx8-based lentiviral vectors have been described previously as selective for catecholaminergic neurons [10], but the artificial promoter PRSx8 is activated by transcription factors Phox2 (a and/or b), which are also expressed in the RTN and A1 neurons, located close to C1 cells [2, 28, 54]. However,

previous studies indicated that the selectivity of the promoter for catecholaminergic neurons depends on the accuracy of virus injections, viral titer, and incubation period [2, 30, 60]. In our experiments, the catecholaminergic neurons were predominantly transduced, but they also included non-catecholaminergic neurons presumed to belong to the RTN [1, 2, 30, 60]. We classified the transduced catecholaminergic neurons as C1 rather than A1 neurons based on their location, because all eYFP and TH double-labeled neurons were located rostral to bregma level  $-13.5$  mm [40]. This classification is based on studies showing that every TH-labeled neuron also labeled with PNMT (enzyme that defines C1 location) is located between  $-11.36$  and  $-13.52$  bregma level [25, 41, 52]. As far as the RTN transduction, we performed control experiments showing that about 20% of the Chr2-expressing neurons were non-catecholaminergic and are located in the RTN region consistent with previous studies [1, 2]. In addition, photostimulation of RTN region in those animals did not elicit changes in breathing (Fig. 3a, c). Therefore, we assumed that the effects described in this study are associated to the transductions of C1 cells.

## Conclusion

We propose that the C1 neurons have a glutamatergic influence on preBötC consistent with their excitatory effects in the spinal cord, the dorsal and ventrolateral pons, and the hypothalamic paraventricular nucleus [22]. Our evidence also suggest that the glutamatergic influence of the C1 neurons on preBötC determines the increase of breathing frequency elicited by photostimulation of C1 cells, and could be modulated by a direct connection to these neurons. In particular, the C1 neurons are strongly activated by acute hypoxia [22], and C1 photostimulation mimics many of the hypoxic effects [9, 22]. In summary, we would like to conclude that the glutamate release from the C1 cell into the preBötC could contribute to the breathing increase during hypoxia.

**Acknowledgements** We would like to acknowledge Dr. Eugenia Constanzi-Strauss for providing the infrastructure that allowed us to perform the virus injection in the brain.

**Authors' contribution** MRML, ACT, and TSM designed research; MRML and LTT performed electrophysiology and anatomy research; MRML and MVGL produced the lentivirus; BES provided material and technical assistance to lentivirus production; MRML and TSM analyzed data; MRML, ACT, and TSM wrote the paper. MRML, LTT, MVGL, BES, ACT, and TSM performed critical review of the manuscript. All authors approved the final version.

**Funding information** This work was supported by the São Paulo Research Foundation (FAPESP; grants 2016/23281-3 to ACT; 2015/23376-1 and 2016/22069-0 to TSM) and the Conselho Nacional de Desenvolvimento Científico e Tecnológico (CNPq; grant 471283/2012-6 to TSM). FAPESP fellowship (2014/07698-6 to MRML) and CNPq fellowship (301219/2016-8 to ACT and 301904/2015-4 to TSM).

## Compliance with ethical standards

**Conflict of interest** The authors declare that they have no conflicts of interest.

## References

- Abbott SBG, Stornetta RL, Fortuna MG, Depuy SD, West GH, Harris TE, Guyenet PG (2009a) Photostimulation of retrotrapezoid nucleus Phox2b-expressing neurons in vivo produces long-lasting activation of breathing in rats. *J Neurosci* 29:5806–5819
- Abbott SBG, Stornetta RL, Socolovsky CS, West GH, Guyenet PG (2009b) Photostimulation of channelrhodopsin-2 expressing ventrolateral medullary neurons increases sympathetic nerve activity and blood pressure in rats. *J Physiol* 587:5613–5631
- Abbott SB, Kanbar R, Bochorishvili G, Coates MB, Stornetta RL, Guyenet PG (2012) C1 neurons excite locus coeruleus and A5 noradrenergic neurons along with sympathetic outflow in rats. *J Physiol* 590:2897–2915
- Abbott SBG, DePuy SD, Nguyen T, Coates MB, Stornetta RL, Guyenet PG (2013) Selective optogenetic activation of rostral ventrolateral medullary catecholaminergic neurons produces cardiorespiratory stimulation in conscious mice. *J Neurosci* 33:3164–3177
- Abbott SBG, Holloway BB, Viar KE, Guyenet PG (2014) Vesicular glutamate transporter 2 is required for the respiratory and parasympathetic activation produced by optogenetic stimulation of catecholaminergic neurons in the rostral ventrolateral medulla of mice in vivo. *Eur J Neurosci* 39:98–106
- Abe C, Inoue T, Inglis MA, Viar KE, Huang L, Ye H, Rosin DL, Stornetta RL, Okusa MD, Guyenet PG (2017) C1 neurons mediate a stress-induced anti-inflammatory reflex in mice. *Nat Neurosci* 20:700–707
- Agassandian K, Shan Z, Raizad M, Sved AF, Card JP (2012) C1 catecholamine neurons form local circuit synaptic connections within the rostroventrolateral medulla of rat. *Neuroscience* 227:247–259
- Bruinstroop E, Cano G, Vanderhorst VGJM, Cavalcante JC, Wirth J, Sena-Esteves M, Saper CB (2012) Spinal projections of the A5, A6 (locus coeruleus), and A7 noradrenergic cell groups in rats. *J Comp Neurol* 520:1985–2001
- Burke PGR, Abbott SBG, Coates MB, Viar KE, Stornetta RL, Guyenet PG (2014) Optogenetic stimulation of adrenergic C1 neurons causes sleep state-dependent cardiorespiratory stimulation and arousal with sighs in rats. *Am J Respir Crit Care Med* 190:1301–1310
- Card JP, Sved JC, Craig B, Raizada M, Vazquez J, Sved AF (2006) Efferent projections of rat rostroventrolateral medulla c1 catecholamine neurons: implications for the central control of cardiovascular regulation. *J Comp Neurol* 499:840–859
- DePuy SD, Kanbar R, Coates MB, Stornetta RL, Guyenet PG (2011) Control of breathing by raphe obscurus serotonergic neurons in mice. *J Neurosci* 31:1981–1990
- DePuy SD, Stornetta RL, Bochorishvili G, Deisseroth K, Witten I, Coates M, Guyenet PG (2013) Glutamatergic neurotransmission between the c1 neurons and the parasympathetic preganglionic neurons of the dorsal motor nucleus of the vagus. *J Neurosci* 33:1486–1497
- Doi A, Ramirez JM (2008) Neuromodulation and the orchestration of the respiratory rhythm. *Respir Physiol Neurobiol* 164:96–104
- Doi A, Ramirez J-M (2010) State-dependent interactions between excitatory neuromodulators in the neuronal control of breathing. *J Neurosci* 30:8251–8262

15. Ellenberger HH, Feldman JL, Zhan W (1990) Subnuclear organization of the lateral tegmental field of the rat. II: catecholamine neurons and ventral respiratory group. *J Comp Neurol* 294:212–222
16. Feldman JL, Del Negro CA (2006) Looking for inspiration: new perspectives on respiratory rhythm. *Nat Rev Neurosci* 7:232–242
17. Feldman JL, McKay LC (2008) Unilateral ablation of pre-Bötzinger complex disrupts breathing during sleep but not wakefulness. *Am J Respir Crit Care Med* 178:89–95
18. Gray PA (1999) Modulation of respiratory frequency by peptidergic input to rhythmogenic neurons in the prebötzinger complex. *Science* 286:1566–1568
19. Gray PA, Janczewski WA, Mellen N, McCrinmon DR, Feldman L (2001) Normal breathing requires preBötzinger complex neurokinin-1 receptor-expressing neurons. *Nat Neurosci* 4:927–930
20. Guyenet PG, Wang H (2001) Pre-Bötzinger neurons with preinspiratory discharges in vivo express NK1 receptors in the rat. *J Neurophysiol* 86:438–446
21. Guyenet PG, Sevigny CP, Weston MC, Stornetta RL (2002) Neurokinin-1 receptor-expressing cells of the ventral respiratory group are functionally heterogeneous and predominantly glutamatergic. *J Neurosci* 22:3806–3816
22. Guyenet PG, Stornetta RL, Bochorishvili G, DePuy SD, Burke PGR, Abbott SBG (2013) C1 neurons: the body's EMTs. *AJP Regul Integr Comp Physiol* 305:R187–R204
23. Hilaire G, Viemari JC, Coulon P, Simonneau M, Bévençut M (2004) Modulation of the respiratory rhythm generator by the pontine noradrenergic A5 and A6 groups in rodents. *Respir Physiol Neurobiol* 143:187–197
24. Hodges MR, Richerson GB (2010) Medullary serotonin neurons and their roles in central respiratory chemoreception. *Respir Physiol Neurobiol* 173:256–263
25. Hokfelt T, Fuxe K, Goldstein M, Johansson O (1974) Immunohistochemical evidence for the existence of adrenaline neurons in the rat brain. *Brain Res* 66:235–251
26. Holloway BB, Stornetta RL, Bochorishvili G, Erisir A, Viar KE, Guyenet PG (2013) Monosynaptic glutamatergic activation of locus coeruleus and other lower brainstem noradrenergic neurons by the c1 cells in mice. *J Neurosci* 33:18792–18805
27. Holloway BB, Viar KE, Stornetta RL, Guyenet PG (2015) The retrotrapezoid nucleus stimulates breathing by releasing glutamate in adult conscious mice. *Eur J Neurosci* 42:2271–2282
28. Hwang DY, Carlezon WA, Isacson O, Kim KS (2001) A high-efficiency synthetic promoter that drives transgene expression selectively in noradrenergic neurons. *Hum Gene Ther* 12:1731–1740
29. Janczewski WA, Tashima A, Hsu P, Cui Y, Feldman JL (2013) Role of inhibition in respiratory pattern generation. *J Neurosci* 33:5454–5465
30. Kanbar R, Stornetta RL, Cash DR, Lewis SJ, Guyenet PG (2010) Photostimulation of Phox2b medullary neurons activates cardiorespiratory function in conscious rats. *Am J Respir Crit Care Med* 182:1184–1194
31. Kang JJ, Liang WH, Lam CS, Huang XF, Yang SJ, Wong-Riley MTT, Fung ML, Liu YY (2017) Catecholaminergic neurons in synaptic connections with pre-Bötzinger complex neurons in the rostral ventrolateral medulla in normoxic and daily acute intermittent hypoxic rats. *Exp Neurol* 287:165–175
32. King TL, Ruyle BC, Kline DD, Heesch CM, Hasser EM (2015) Catecholaminergic neurons projecting to the paraventricular nucleus of the hypothalamus are essential for cardiorespiratory adjustments to hypoxia. *Am J Phys Regul Integr Comp Phys* 309:R721–R731
33. Koshiya N, Huangfu D, Guyenet PG (1993) Ventrolateral medulla and sympathetic chemoreflex in the rat. *Brain Res* 609:174–184
34. Kubin L, Alheid GF, Zuperku EJ, McCrinmon DR (2006) Central pathways of pulmonary and lower airway vagal afferents central pathways of pulmonary and lower airway vagal afferents. *J Appl Physiol* 101:618–627
35. Malheiros-Lima MR, Takakura AC, Moreira TS (2017) Depletion of rostral ventrolateral medullary catecholaminergic neurons impairs the hypoxic ventilatory response in conscious rats. *Neuroscience* 351:1–14
36. Menuet C, Le S, Dempsey B, Connelly AA, Kamar JL, Jancovski N, Bassi JK, Walters K, Simms AE, Hammond A, Fong AY, Goodchild AK, McMullan S, Allen AM (2017) Excessive respiratory modulation of blood pressure triggers hypertension. *Cell Metab* 25:739–748
37. Moraes DJ, Zoccal DB, Machado BH (2012) Sympathoexcitation during chemoreflex active expiration is mediated by L-glutamate in the RVLM/Botzinger complex of rats. *J Neurophysiol* 108:610–623
38. Moreira TS, Sato MA, Takakura ACT, Menani JV, Colombari E (2005) Role of pressor mechanisms from the NTS and CVLM in control of arterial pressure. *Am J Phys Regul Integr Comp Phys* 289:R1416–R1425
39. Oliveira LM, Moreira TS, Kuo FS, Mulkey DK, Takakura AC (2016)  $\alpha$ 1- and  $\alpha$ 2-adrenergic receptors in the retrotrapezoid nucleus differentially regulate breathing in anesthetized adult rats. *J Neurophysiol* 116:1036–1048
40. Paxinos G, Watson C (2007) The rat brain in stereotaxic coordinates, 6th edn. Elsevier Academic Press, San Diego
41. Phillips JK, Goodchild AK, Dubey R, Sesiashvili E, Takeda M, Chalmers J, Pilowsky PM, Lipski J (2001) Differential expression of catecholamine biosynthetic enzymes in the rat ventrolateral medulla. *J Comp Neurol* 432:20–34
42. Pilowsky PM, Jiang C, Lipski J (1990) An intracellular study of respiratory neurons in the rostral ventrolateral medulla of the rat and their relationship to catecholamine-containing neurons. *J Comp Neurol* 301:604–617
43. Ramirez JM (2015) The integrative role of the sigh in psychology, physiology, pathology, and neurobiology. *Prog Brain Res* 209:91–129
44. Ramirez J-M, Richter DW (1996) The neuronal mechanisms of respiratory rhythm generation. *Curr Opin Neurobiol* 6:817–825
45. Schreihofer AM, Guyenet PG (1997) Identification of C1 and nonadrenergic presympathetic neurons (PSNS) of rostral ventrolateral medulla (RVLM) by juxtacellular label of single recorded cells “in vivo” in rat. *FASEB J* 11:524–536
46. Schwarzacher SW, Rüb U, Deller T (2011) Neuroanatomical characteristics of the human pre-Bötzinger complex and its involvement in neurodegenerative brainstem diseases. *Brain* 134:24–35
47. Silva TM, Takakura AC, Moreira TS (2016) Acute hypoxia activates hypothalamic paraventricular nucleus-projecting catecholaminergic neurons in the C1 region. *Exp Neurol* 285:1–11
48. Smith JC, Ellenberger HH, Ballanyi K, Richter DW, Feldman JL (1991) Pre-Bötzinger complex: a brainstem region that may generate respiratory rhythm in mammals. *Science* 254:726–729
49. Smith JC, Abdala AP, Borgmann A, Rybak IA, Paton JF (2014) Brainstem respiratory networks: building blocks and microcircuits. *Trends Neurosci* 36:152–162
50. Solomon IC, Edelman NH, Neubauer JA (1999) Patterns of phrenic motor output evoked by chemical stimulation of neurons located in the pre-Bötzinger complex in vivo. *J Neurophysiol* 81:1150–1161
51. Stornetta RL (2009) Neurochemistry of bulbohypospinal presympathetic neurons of the medulla oblongata. *J Chem Neuroanat* 38:222–230
52. Stornetta RL, Akey PJ, Guyenet PG (1999) Location and electrophysiological characterization of rostral medullary adrenergic neurons that contain neuropeptide Y mRNA in rat medulla. *J Comp Neurol* 415:482–500
53. Stornetta RL, Sevigny CP, Guyenet PG (2002) Vesicular glutamate transporter DNPI/VGLUT2 mRNA is present in C1 and several other groups of brainstem catecholaminergic neurons. *J Comp Neurol* 444:191–206

54. Stornetta RL, Moreira TS, Takakura AC, Kang BJ, Chang DA, West GH, Brunet JF, Mulkey DK, Bayliss DA, Guyenet PG (2006) Expression of Phox2b by brainstem neurons involved in chemosensory integration in the adult rat. *J Neurosci* 26:10305–10314
55. Stornetta RL, Inglis MA, Viar KE, Guyenet PG (2016) Afferent and efferent connections of C1 cells with spinal cord or hypothalamic projections in mice. *Brain Struct Funct* 221:4027–4044
56. Takakura ACT, Moreira TS, Colombari E, West GH, Stornetta RL, Guyenet PG (2006) Peripheral chemoreceptor inputs to retrotrapezoid nucleus (RTN) CO<sub>2</sub>-sensitive neurons in rats. *J Physiol* 572:503–523
57. Viemari JC (2008) Noradrenergic modulation of the respiratory neural network. *Respir Physiol Neurobiol* 164:123–130
58. Viemari J-C, Ramirez J-M (2006) Norepinephrine differentially modulates different types of respiratory pacemaker and nonpacemaker neurons. *J Neurophysiol* 95:2070–2082
59. Viemari J-C, Garcia AJ, Doi A, Elsen G, Ramirez J-M (2013) B-noradrenergic receptor activation specifically modulates the generation of sighs in vivo and in vitro. *Front Neural Circuits* 7:1–14
60. Wenker IC, Abe C, Viar KE, Stornetta DS, Stornetta RL, Guyenet PG (2017) Blood pressure regulation by the rostral ventrolateral medulla in conscious rats: effects of hypoxia, hypercapnia, baroreceptor denervation and anesthesia. *J Neurosci* 37:4565–4583